

# GNSS Measurement-Based Context Recognition for Vehicle Navigation using Gated Recurrent Unit

Sheng Liu, *School of Mathematics and Computational Science, Xiangtan University, Xiangtan, 411105, China*  
Zhiqiang Yao, *School of Automation and Electronic Information, Xiangtan University, Xiangtan, 411105, China*  
Xuemeng Cao, *School of Automation and Electronic Information, Xiangtan University, Xiangtan, 411105, China*  
Xiaowen Cai, *School of Automation and Electronic Information, Xiangtan University, Xiangtan, 411105, China*

## BIOGRAPHY

**Sheng Liu** received his B.S. degree in Electronic Information Science and Technology from Xiangtan University in June 2018. He is currently a Ph.D. candidate at the School of Mathematics and Computational Science in Xiangtan University. His research interests include optimization algorithms in context-adaptive navigation and scenario recognition for vehicle navigation.

**Zhiqiang Yao** received his master's and doctorate degrees in engineering from South China University of Technology in 2004 and 2010, respectively. He is currently the dean (professor) of the School of Automation and Electronic Information at Xiangtan University. He serves as the director of the Key Laboratory of Intelligent Reliable Navigation and Positioning of Hunan Province and holds the position of director at the China Satellite Navigation and Positioning Association. His research interests include multi-sensor integrated navigation and context-adaptive navigation.

**Xuemeng Cao** received his B.S. degree in Electronic Information Engineering from Xiangtan University in 2021. He is currently engaged in the pursuit of a master's degree in the same field. His research focuses on scenario recognition for navigation and multirate multisensor data fusion.

**Xiaowen Cai** received the Ph.D. degree in optical engineering with Beihang University, Beijing, China, in 2020. Her research interests are related to inertial navigation and integrated navigation.

## ABSTRACT

Recent years, people have put forward higher and higher requirements for context-adaptive navigation (CAN). CAN system realizes seamless navigation in complex environments by recognizing the ambient surroundings of vehicles, and it is crucial to develop a fast, reliable, and robust navigational context recognition (NCR) method to enable CAN systems to operate effectively. Environmental context recognition based on Global Navigation Satellite System (GNSS) measurements has attracted widespread attention due to its low cost because it does not require additional infrastructure. The performance and application value of NCR methods depend on three main factors: context categorization, feature extraction, and classification models. In this paper, a fine-grained context categorization framework comprising seven environment categories (open sky, tree-lined avenue, semi-outdoor, urban canyon, viaduct-down, shallow indoor, and deep indoor) is proposed, which currently represents the most elaborate context categorization framework known in this research domain. To improve discrimination between categories, a new feature called the  $C/N_0$ -weighted azimuth distribution factor, is designed. Then, to ensure real-time performance, a lightweight gated recurrent unit (GRU) network is adopted for its excellent sequence data processing capabilities. A dataset containing 59,996 samples is created and made publicly available to researchers in the NCR community on Github. Extensive experiments have been conducted on the dataset, and the results show that the proposed method achieves an overall recognition accuracy of 99.41% for isolated scenarios and 94.95% for transition scenarios, with an average transition delay of 2.14 seconds.

## I. INTRODUCTION

With the rapid development of autonomous driving, integrated navigation and seamless positioning ( $\circ$ ), people have put forward higher and higher requirements for context-adaptive navigation (CAN). Vehicle navigation and positioning are highly dependent on the surrounding environments, and no single technology can adapt to all operating environments. For instance, GNSS-based navigation performs well in open environments with few or no signal obstructions and interference; in semi-open environments, especially in urban canyons, shadow matching (Groves, 2011) and 3DMA (Adjrjad & Groves, 2016) can be used to assist GNSS localization; in indoor and severe GNSS-denied environments, navigation methods based on cellular signal, WiFi, Bluetooth, UWB and INS are mainly adopted ( $\circ$ ). CAN systems achieve seamless navigation in complex environments by recognizing

the ambient surroundings of the vehicle. Therefore, it is crucial to develop a fast, reliable, and robust navigational context recognition (NCR) method to enable CAN systems' effective operation.

The effectiveness and practicality of NCR methods mainly rely on three key factors: context categorization, feature extraction, and classification model.

First, context categorization proposed for general or other purposes may not be suitable for CAN. For specific navigation applications, such as autonomous driving, a dedicated context categorization framework should be proposed based on the navigation requirements and the characteristics of different contexts. To the best of our knowledge, the existing literature () mainly divides the environments under consideration into four categories or less, namely deep indoor, shallow indoor, semi-outdoor, and open-sky. Such context categorization methods are too coarse for vehicle navigation to be used in CAN. Second, selecting the appropriate signal or sensor types and extracting the proper features are the cornerstone of NCR. Among the various types of sensors or signals for NCR, the recognition scheme based on GNSS signals is widely used due to its universality, high availability, and low cost (Feriol et al., 2020). In terms of identification features, researchers have proposed a large number of useful features to distinguish various types of context, such as the mean and variance of GNSS signal's carrier-to-noise ratio ( $C/N_0$ ), satellite blocking coefficient, and fluctuation coefficient (Y. Wang et al., 2019). However, when more elaborate classifications are required, new features need to be devised. Last, determining the appropriate classification model is crucial to achieve fast, accurate, and robust context recognition performance. Existing classification models mainly include fuzzy inference (Zadeh, 1996), support vector machine (SVM) (Suthaharan, 2016), and long-short term memory (LSTM) (Sherstinsky, 2020). With the development of big data technology, large-scale parallel computing, and the popularity of graphics processing unit (GPU) devices, deep learning has emerged as a promising field, with algorithms such as Convolutional Neural Networks (CNN, Dai et al., 2022), Transformers (Vaswani et al., 2017) and Gated Recurrent Unit (GRU, Chung et al., 2014).

For the GNSS measurement-based methods, a classical approach is called SatProbe (Chen & Tan, 2017), which determines the indoor/outdoor status using only the number of visible GPS satellites. Although this method turn out to be efficient, its binary classification needs improvement for applicability in broader contexts. Xia et al. (2020) used an LSTM network, to divide environments into four categories (deep indoors, shallow indoors, semi-outdoors, and open outdoors) based on smartphone GNSS measurements. They achieved an overall accuracy of 98.65% and a maximum scenario transition recognition delay of 3s. However, the constructed features suffered from redundancy, leading to unnecessary computations. Moreover, most smartphones' GNSS modules have a sampling rate of only 1Hz, which hampers the responsiveness to scenario transition. More recently, Dai et al. (2022) proposed a grid-based recognition approach that utilizes GNSS measurements such as pseudorange, Doppler shift, and  $C/N_0$ . They represented the GNSS measurements with Voronoi diagrams and fed them into CNN networks, and achieved an accuracy of 99.92%. However, the categorization is not specifically designed for vehicle navigation. In addition, classifying images generally incurs higher computational overhead compared to numerical samples.

To summarize, NCR faces three main challenges, namely categorization framework, feature extraction, and classification models. In response to these challenges, we dedicate to propose an elaborate categorization framework, and implement recognition by using a lightweight network with appropriate features. The main contributions of this paper are:

- A novel fine-grained context categorization framework was proposed based on the characteristics of different environments and their corresponding integrated navigation methods, which currently represents the most elaborate context categorization framework known in this research field.
- To improve discrimination between categories, a new feature called the  $C/N_0$ -weighted azimuth distribution factor was designed.
- To ensure real-time performance, a lightweight GRU network was adopted for its excellent sequence data processing capabilities.
- A corresponding dataset containing 59,996 samples was created, which will serve as a valuable resource for the NCR research community.

## II. METHODOLOGY

### 1. Context Categorization Framework

Targeting the navigation of autonomous vehicles in urban areas, the environments that they traverse are diverse. The selection of environmental category elements should be based on the available sensor types and the quality of wireless signal reception. The most used four-category framework (deep indoors, shallow indoors, semi-outdoors, and open outdoors) provide a basic skeleton, but it's not dedicated designed for vehicle navigation. We expand it by adding three other distinct categories and propose a fine-grained context categorization framework based on the characteristics of different environments and their corresponding integrated navigation methods.

Table 1 shows the definitions, signal characteristics, and corresponding integrated navigation methods for each environmental

**Table 1:** Context categorization framework based on the characteristics of different environments and their corresponding integrated navigation methods.

categories	descriptions	GNSS signal characteristics	integrated navigation methods
open sky	position with an elevation angle of less than $15^\circ$ from the top edge of most surrounding buildings	all GNSS signals in the sky are well received with strong $C/N_0$	GNSS
tree-lined avenue	leaves on both sides of the road almost cover the sky above the road	signal strength experiences some degree of attenuation	GNSS, LTE/5G, INS
semi-outdoor	building exists on one side and the elevation of its top edge is greater than $45^\circ$	signals at low and medium elevation angles on one side are blocked	GNSS, WiFi, LTE/5G, INS
urban canyon	a large number of super high-rise buildings on both sides of the road	signals come from high elevation on the top	GNSS Shadow matching, 3DMA, INS
viaduct-down	position located under a viaduct	signals come from low elevation on both sides	GNSS, UWB, INS
shallow indoor	position located indoors and near an outside window	weak GNSS signals coming from the side of the window	GNSS, WiFi, INS
deep indoor	position located indoors and away from an outside window	almost no GNSS signal available	WiFi, Bluetooth, UWB, INS

types in the proposed seven-category framework. It includes seven categories: open sky, tree-lined avenues, semi-outdoor, urban canyons, viaduct-down, shallow indoor, and deep indoor, which currently represents the most elaborate context categorization framework known in this research domain. For example, the semi-outdoor environment refers to a location where there is a building exists on one side and the elevation of its top edge is greater than  $45^\circ$ . Signals coming from elevations lower than this angle on that side are blocked. The navigation solution for the semi-outdoor environment can be achieved by the integration of GNSS, WiFi, cellular signals and/or INS.

The seven-category framework significantly improves the environmental coverage, but it also increases the difficulty of inter-class discrimination. For example, in the four-category framework, there is no category for viaduct-down, and according to the signal characteristics, it should be classified as a shallow indoor environment. However, how to distinguish between viaduct-down and shallow indoor in the seven-category framework? New features need to be designed to solve the inter-class confusion problem brought by the extended framework.

## 2. Feature Design/Selection

Here we show the satellite skyplots (Figure 1) of the GNSS signals received in three typical scenarios (open-sky, viaduct-down and shallow indoor) often encountered in CAN, with green representing satellites with strong  $C/N_0$  values, blue for weak  $C/N_0$  values, and red for unavailable satellites. Two key observations can be made from them:

- Firstly, relying solely on statistical features of satellites'  $C/N_0$  and number is insufficient to effectively distinguish between each type of environment;

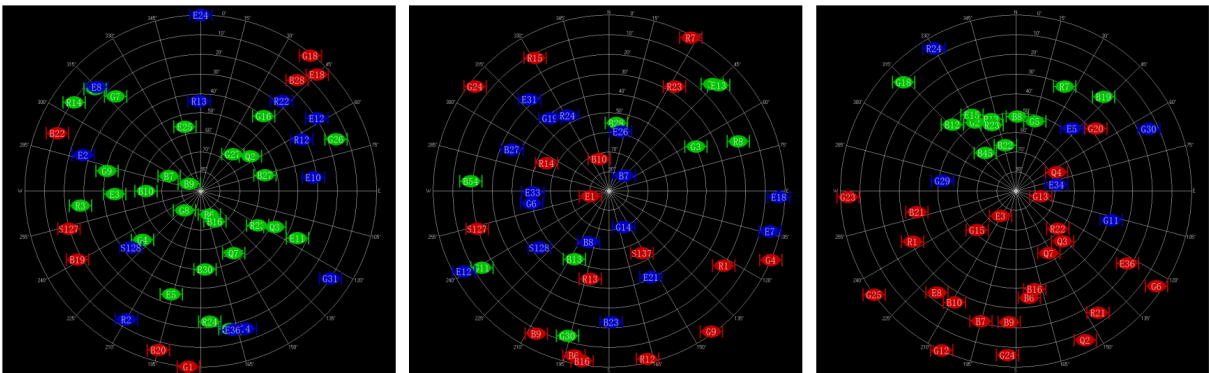


**Figure 1:** Satellite skyplots of open-sky (left), viaduct-down (middle) and shallow indoor (right) environments, where green represents satellites with strong  $C/N_0$  values, blue for weak values, red for unavailable satellites.

- Secondly, there is a noticeable "semi" nature exhibited in certain environments, which can potentially be utilized as a distinguishing factor.

The problem is how to definitely describe this "semi" nature.

Hence, a new feature called the  $C/N_0$ -weighted azimuth distribution factor ( $r$ ) is designed to improve discrimination between categories. As shown in Figure 2, we denote  $b$  as the bisector. It divides the entire skyplot into two sectors, namely  $A_{b1}$  and  $A_{b2}$ , respectively. Mathematically,  $r$  can be obtained by solving the optimization problem described in equation (1).

$$r = \max_{b \in [0, 360^\circ)} r_b$$

$$s.t. \begin{cases} r_b = \frac{C/N_{0b1}}{C/N_{0b2}} \\ C/N_{0bi} = \sum_{a_j \in A_{bi}} c_j, i = 1, 2, j = 1, \dots, N \\ A_{b1} = \{a | b \leq a < b + 180^\circ \text{ or } 0^\circ \leq a < b - 180^\circ\} \\ A_{b2} = \{a | b - 180^\circ \leq a < b \text{ or } b + 180^\circ \leq a < 360^\circ\} \end{cases} \quad (1)$$

where  $a_j$  and  $c_j$  denote the azimuth and  $C/N_0$  measurement of the  $j$ -th available satellite,  $A_{b1}$  and  $A_{b2}$  are clockwise and counterclockwise ranges of  $180^\circ$  start from the bisector  $b$ , respectively. Calculate the sum of  $C/N_0$  of all available satellites in  $A_{b1}$  and  $A_{b2}$ , respectively, and compute their ratio  $r_b$ . When  $b$  varies in  $[0, 360^\circ)$ , the maximum value of  $r_b$  is taken as the feature of this epoch.

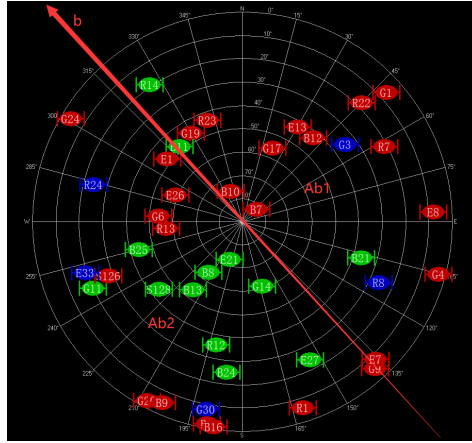


**Figure 2:** Example of a satellite skyplot where  $b$  is the bisector,  $A_{b1}$  and  $A_{b2}$  are clockwise and counterclockwise ranges of  $180^\circ$ .

This new feature significantly improves the discrimination between different categories, especially between shallow indoor and viaduct-down. When the vehicle is in a shallow indoor environment, most of the strong GNSS signals are received from the side with windows, which will lead to a high value of  $r$  (far greater than 1). On the contrary, when the vehicle is under a viaduct, the number and strength of GNSS signals from both sides are not much different, which will result in an  $r$  value close to 1. The classification model will learn this difference during the training phase and apply it during the identification phase.

In addition to the proposed feature  $r$ , the 10-dimensional feature vector used in this paper also includes the number of visible satellites, and the mean, standard deviation, maximum, minimum, skewness, kurtosis, median, and interquartile range of satellite  $C/N_0$  within an epoch. To ensure real-time performance, a lightweight GRU network is adopted for its excellent sequence data processing capabilities. Details of the implementation of GRUs can be found in (Chung et al., 2014).

### III. EXPERIMENTS AND RESULTS

#### 1. Data Collection

To validate the performance of the proposed method, extensive field experiments were conducted. We collected the NMEA-0183 (National Marine Electronics Association) samples using an u-blox F9K receiver (as shown in Figure 3) with a sampling frequency of 5 Hz. Some key parameters of the used receiver are provided in Table 2.

The dataset consists of a total of 59,996 samples, as described in Table 3. Each set of data lasts approximately 4 minutes, equivalent to around 1200 samples. And to ensure the broad representativeness, they were collected by different volunteers

at different locations and time for each type of environment. In order to facilitate further research, we have made this dataset publicly available on Github (Liu, 2023) for researchers in the NCR community. It will serve as a benchmark for this research field.



**Figure 3:** U-blox F9K receiver and multi-band active GNSS antenna.

**Table 2:** Parameters of the receiver U-blox F9K

Items	Parameters
Constellations	GLONASS/Galileo/ GPS/BDS/QZSS
Signal frequencies	L1C/A, L2C, L1OF, L2OF, E1-B/C, E5b, B1I, B2I
Max output rate	100 Hz
Tracking Sensitivity	-158dbm
Protocols	NMEA, UBX, RTCM

**Table 3:** Number of sets and samples for each scenario.

Categories	open sky	tree-lined avenue	semi-outdoor	urban canyon	under-viaduct	shallow indoor	deep indoor
Number of sets	7	7	7	7	7	7	7
Number of samples	8631	8577	8803	8507	8445	8546	8487

## 2. Ablation Experiment

The ablation experiment was designed to validate the performance of the proposed new feature (the  $C/N_0$ -weighted azimuth distribution factor  $r$ ). First, consider the 11-dimensional feature vector  $x_t$  proposed in (Xia et al., 2020) :

$$x_t = \{num, sum, mean, std, max, min, range, skewness, kurtosis, median, iqr\} \quad (2)$$

There are two deterministic correlations between the elements within this vector:

$$mean = sum/num, range = max - min.$$

Remove  $sum$  and  $range$  from  $x_t$ , resulting in a 9-dimensional feature vector, denoted as

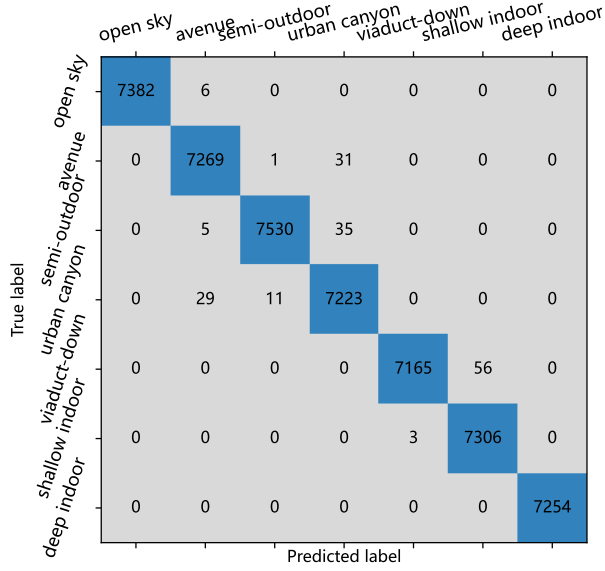
$$y_t = \{num, mean, std, max, min, skewness, kurtosis, median, iqr\}. \quad (3)$$

Next, by incorporating the proposed feature  $r$ , the feature vector  $z_t$  is obtained:

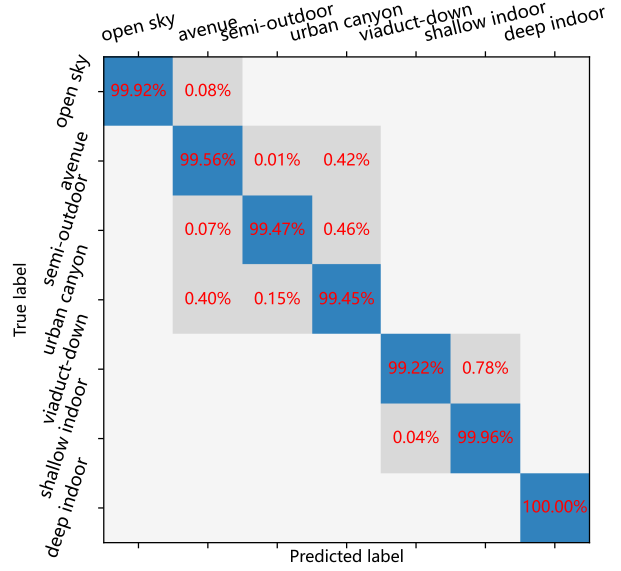
$$z_t = \{num, mean, std, max, min, skewness, kurtosis, median, iqr, ratio\}. \quad (4)$$

Then feed  $y_t$  and  $z_t$  into the GRU network, and evaluate their performance. To train a recognition model, many hyperparameters need to be set and tuned. Here we present the key parameters selected after trial and error. A network with two hidden layers, each containing 180 GRU neurons, was adopted. To capture the temporal correlation of scenario transitions, the length of the sliding window in the temporal domain was set to 6 samples. The max training epochs was set to 35, and the batch size was set to 256, resulting a iteration number of about 7000. The learning rate was set to  $5.0E-5$ .

The classification confusion matrices of the model trained based on features  $y_t$  and  $z_t$  are shown in Figure 4 and Figure 5, respectively. It can be observed that when trained based on  $y_t$ , the model tends to confuse three groups of environments. And they lead to a training accuracy of only 99.66%. The most severe confusion occurs between viaduct-down and shallow indoor. When the vehicle passes between two piers under a viaduct, the semi-enclosed space obstructs the GNSS signal, reducing the number and strength of the received satellites, resulting in performance similar to entering a shallow indoor environment. However, with the new feature introduced in  $z_t$ , these similarities or confusions have been significantly reduced, or even eliminated altogether. As a result, we achieved an overall accuracy of 99.94% , as shown in Fig. 5. As mentioned before, this can be attributed to the fact that distinct value of the proposed feature are obtained in the former confused environments.

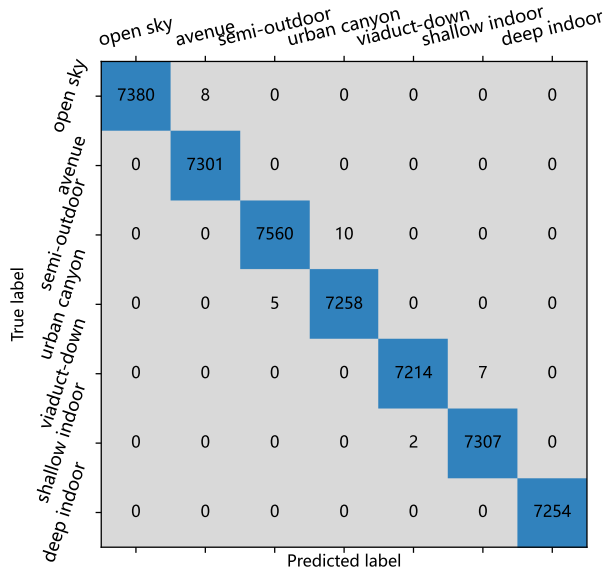


(a) Confusion matrix (sample numbers)

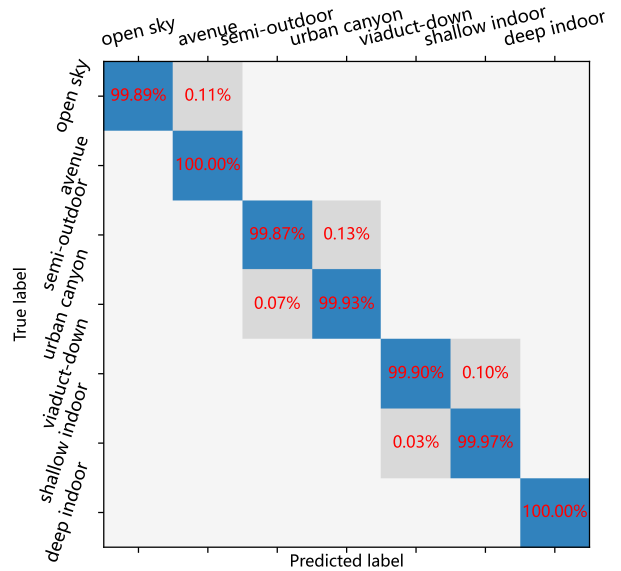


(b) Confusion matrix (sample percentages)

Figure 4: The confusion matrices of the model based on features  $y_t$ , overall accuracy: 99.66%.



(a) Confusion matrix (sample numbers)



(b) Confusion matrix (sample percentages)

Figure 5: The confusion matrices of the model based on features  $z_t$ , overall accuracy: 99.94%

### 3. Comparison Experiments

In the subsequent experiments, we compare the proposed GRU-based method with the SVM-based method on an isolated testset. The SVM-based method uses temporal filtering (Y. Wang et al., 2019) with a fixed sliding window of 6 samples and it is labeled as "SVM-TF". They are both trained or learned using the proposed  $z_t$  feature vectors. Their confusion matrices on the isolated test set are shown in Table 4 and 5, respectively. The GRU-based method has a high recognition accuracy of 99.41%, which slightly outperforms the SVM-TF-based method, 99.35%. This can be attributed to the excellent characterization ability of the proposed  $z_t$  in different environments, as well as the strong expression ability of the models.

To evaluate the performance in transition scenarios, we conducted 4 sets of comparative experiments, as shown in Figure

**Table 4:** Confusion matrix of the proposed GRU-based method on the isolated testset, overall accuracy: 99.41%. Labels 0 to 6 represent 'open sky', 'tree-lined avenues', 'semi-outdoor', 'urban canyon', 'viaduct-down', 'shallow indoor' and 'deep indoor', respectively. The same labeling applies in the subsequent tables.

Actual	Predicted						
	0	1	2	3	4	5	6
<b>0</b>	<b>100.00%</b>	0.00%	0.00%	0.00%	0.00%	0.00%	0.00%
<b>1</b>	0.00%	<b>100.00%</b>	0.00%	0.00%	0.00%	0.00%	0.00%
<b>2</b>	0.00%	0.00%	<b>99.67%</b>	0.33%	0.00%	0.00%	0.00%
<b>3</b>	0.00%	0.00%	0.00%	<b>98.51%</b>	1.49%	0.00%	0.00%
<b>4</b>	0.00%	0.00%	0.00%	0.00%	<b>97.90%</b>	2.10%	0.00%
<b>5</b>	0.00%	0.00%	0.25%	0.00%	0.00%	<b>99.75%</b>	0.00%
<b>6</b>	0.00%	0.00%	0.00%	0.00%	0.00%	0.00%	<b>100.00%</b>

**Table 5:** Confusion matrix of the SVM-TF-based method on the isolated testset, overall accuracy: 99.35%.

Actual	Predicted						
	0	1	2	3	4	5	6
<b>0</b>	<b>100.00%</b>	0.00%	0.00%	0.00%	0.00%	0.00%	0.00%
<b>1</b>	0.00%	<b>100.00%</b>	0.00%	0.00%	0.00%	0.00%	0.00%
<b>2</b>	0.00%	0.00%	<b>99.50%</b>	0.50%	0.00%	0.00%	0.00%
<b>3</b>	0.00%	0.00%	0.00%	<b>98.68%</b>	1.32%	0.00%	0.00%
<b>4</b>	0.00%	0.00%	0.00%	0.00%	<b>97.90%</b>	2.10%	0.00%
<b>5</b>	0.00%	0.00%	0.67%	0.00%	0.00%	<b>99.33%</b>	0.00%
<b>6</b>	0.00%	0.00%	0.00%	0.00%	0.00%	0.00%	<b>100.00%</b>

6-9. The overall average recognition accuracy of the GRU-based method in these five transition scenarios is 94.95%, which is significantly higher than the 90.99% achieved by the SVM-TF-based method. This is because the former has already taken the temporal relationship of the samples into consideration during the learning stage, while the latter only applies a temporal filtering to the recognition results of single moments. The 2<sup>nd</sup> experiment follows the opposite process of the 1<sup>st</sup> one. For the GRU-based method, although both experiments are conducted in the same route, the accuracy and delay in the 2<sup>nd</sup> one are inferior to those in the 1<sup>st</sup> one. This is because in the 1<sup>st</sup> experiment, the environmental changes follow a gradual decrease in skyvisibility, and the receiver can immediately detect the decrease in signal quantity and quality. Instead, in the 2<sup>nd</sup> experiment, as the skyvisibility increases, the receiver needs some time to acquire and track the newly visible satellites. The same phenomenon can be observed in the 1<sup>st</sup> and 2<sup>nd</sup> halves of the 3<sup>rd</sup> experiment, when the vehicle crossing the viaduct-down environment. Beside, there are a total of 10 transitions in these 4 experiments, with an average delays of 2.14s, demonstrating the real-time performance of the proposed method.

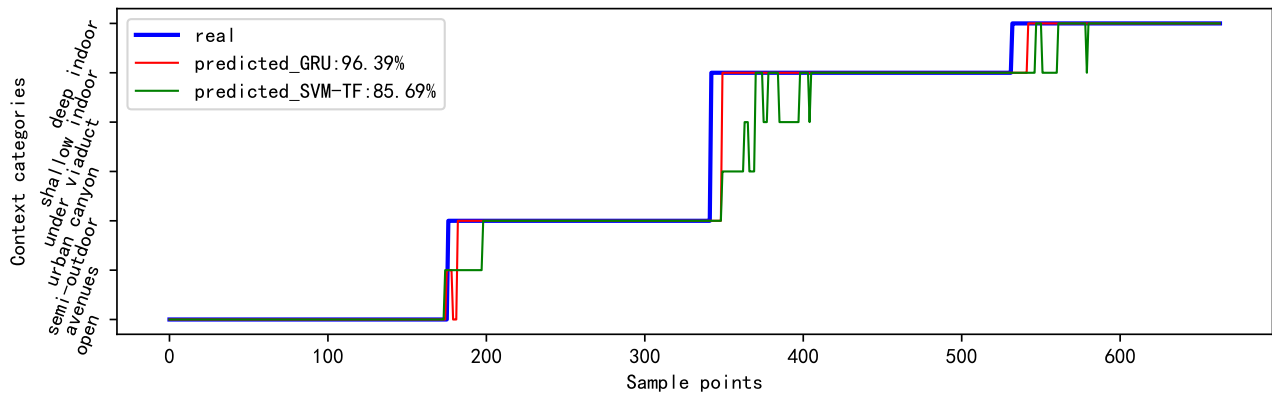


**Figure 6:** Transition scenario 1: open sky→semi-outdoor→shallow indoor→deep indoor

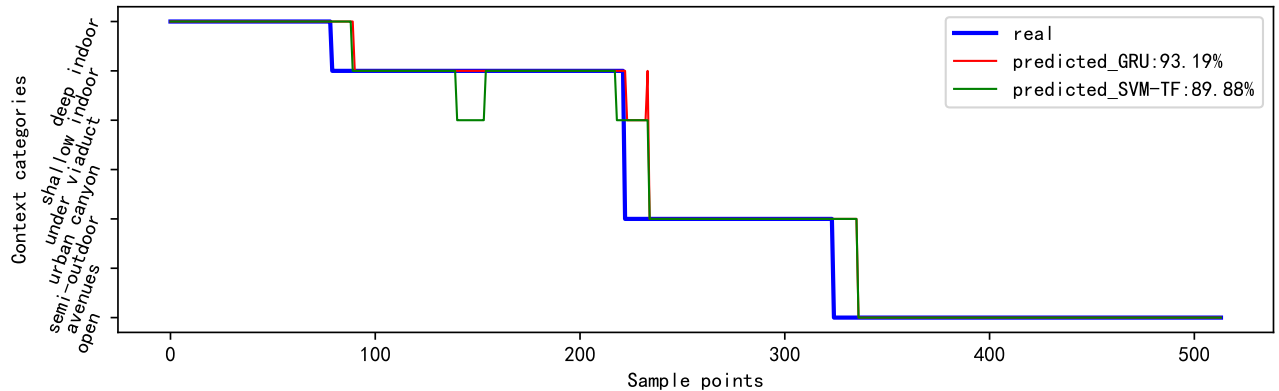


Figure 7: Transition scenario 2: deep indoor → shallow indoor → semi-outdoor → open sky

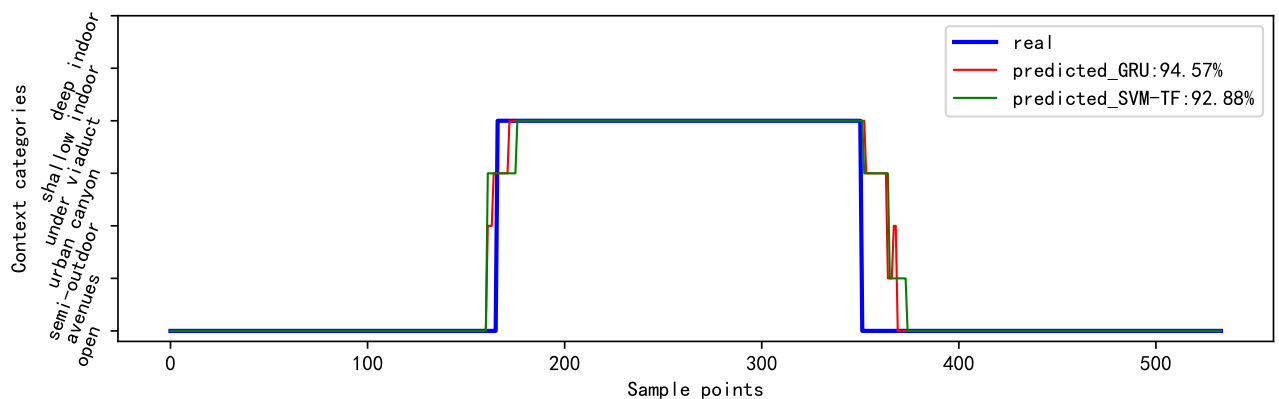


Figure 8: Transition scenario 3: open sky → viaduct-down → open sky

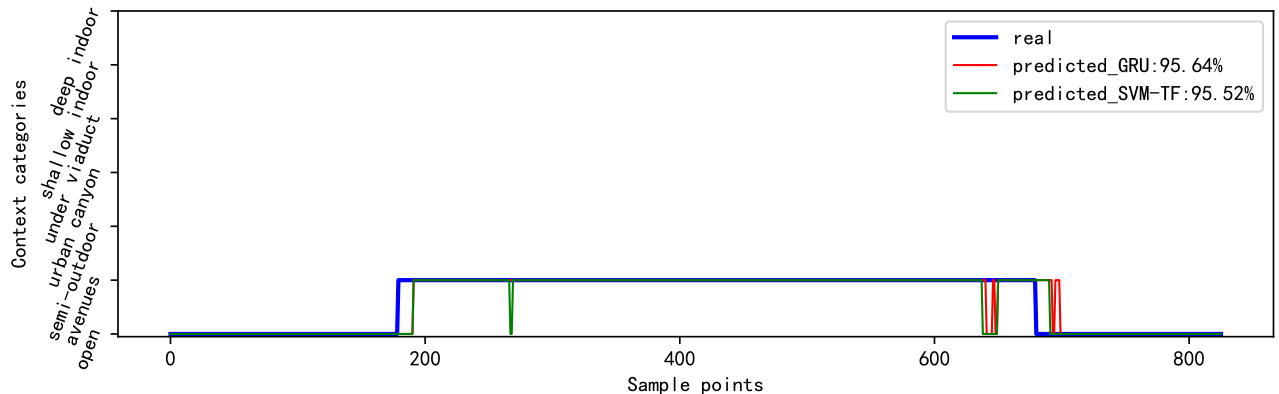


Figure 9: Transition scenario 4: open sky → tree-lined avenue → open sky

#### IV. CONCLUSIONS

In this paper, we studied the NCR approach for context-adaptive navigation. We proposed a new and fine-grained context categorization framework based on the characteristics of different environments and their corresponding integrated navigation methods, which is currently the most elaborate context categorization framework known. A new feature called the satellite azimuth distribution factor weighted by carrier-to-noise ratio  $r$ , was designed, which significantly improves the discrimination between different categories. To ensure real-time performance, a GRU network was adopted for its excellent sequence data processing capability. A corresponding data set was created, which will serve as a valuable resource for the NCR research community. Experiments results show that the proposed method is superior in terms of both recognition accuracy and



computational complexity to the state-of-the-art. Overall, this work has significant implications for the development of context-adaptive navigation systems, which have the potential to greatly enhance user experience and safety in navigation applications.

## ACKNOWLEDGMENTS

This work was supported in part by the National Key R&D Program of China under Grant No. 2020YFA0713502 and in part by Hunan Provincial Innovation Foundation For Postgraduate with Grant No. CX20210610. We are grateful to the High Performance Computing Platform of Xiangtan University for assistance with the computations in training stage.

## REFERENCES

- Adjrad, M., & Groves, P. D. (2016). Intelligent urban positioning using shadow matching and gnss ranging aided by 3d mapping. *Proceedings of the 29th International Technical Meeting of the Satellite Division of The Institute of Navigation (ION GNSS+ 2016)*, 534–553.
- Chen, K., & Tan, G. (2017). Satprobe: Low-energy and fast indoor/outdoor detection based on raw gps processing. *IEEE INFOCOM 2017 - IEEE Conference on Computer Communications*, 1–9. <https://doi.org/10.1109/INFOCOM.2017.8057095>
- Chung, J., Gulcehre, C., Cho, K., & Bengio, Y. (2014). Empirical evaluation of gated recurrent neural networks on sequence modeling. *arXiv preprint arXiv:1412.3555*.
- Dai, Z., Zhai, C., Li, F., Chen, W., Zhu, X., & Feng, Y. (2022). Deep learning-based scenario recognition with gnss measurements on smartphones. *IEEE Sensors Journal*, 1–1. <https://doi.org/10.1109/JSEN.2022.3230213>
- Do Nascimento, L. V., Machado, G. M., Maran, V., & de Oliveira, J. P. M. (2021). Context recognition and ubiquitous computing in smart cities: a systematic mapping. *Computing*, 103(5), 801–825. <https://doi.org/10.1007/s00607-020-00878-7>
- Feriol, F., Vivet, D., & Watanabe, Y. (2020). A review of environmental context detection for navigation based on multiple sensors. *Sensors (Switzerland)*, 20(16), 1–30. <https://doi.org/10.3390/s20164532>
- Gao, H., & Groves, P. D. (2018). Environmental Context Detection for Adaptive Navigation using GNSS Measurements from a Smartphone. *Navigation, Journal of the Institute of Navigation*, 65(1), 99–116. <https://doi.org/10.1002/navi.221>
- Groves, P. D. (2011). Shadow matching: A new GNSS positioning technique for urban canyons. *Journal of Navigation*, 64(3), 417–430. <https://doi.org/10.1017/S0373463311000087>
- Kassas, Z. Z. M., Khalife, J., Shamaei, K., & Morales, J. (2017). I hear, therefore i know where i am: Compensating for gnss limitations with cellular signals. *IEEE Signal Processing Magazine*, 34(5), 111–124.
- Liu, S. (2023). Nmea dataset for navigation context recognition:<https://github.com/liusheng2020/nmeadatasetnrcr> [Accessed: 2023-03-01].
- Sherstinsky, A. (2020). Fundamentals of recurrent neural network (rnn) and long short-term memory (lstm) network. *Physica D: Nonlinear Phenomena*, 404, 132306.
- Suthaharan, S. (2016). Support vector machine. In *Machine learning models and algorithms for big data classification* (pp. 207–235). Springer.
- Vaswani, A., Shazeer, N., Parmar, N., Uszkoreit, J., Jones, L., Gomez, A. N., Kaiser, L., & Polosukhin, I. (2017). Attention is all you need. *Advances in neural information processing systems*, 30.
- Wang, C., Xu, A., Sui, X., Hao, Y., Shi, Z., & Chen, Z. (2022). A seamless navigation system and applications for autonomous vehicles using a tightly coupled GNSS/UWB/INS/map integration scheme. *Remote Sensing*, 14(1). <https://doi.org/10.3390/rs14010027>
- Wang, Y., Liu, P., Liu, Q., Adeel, M., Qian, J., Jin, X., & Ying, R. (2019). Urban environment recognition based on the gnss signal characteristics. *Navigation*, 66, 211–225.
- Xia, Y., Pan, S., Gao, W., Yu, B., Gan, X., Zhao, Y., & Zhao, Q. (2020). Recurrent neural network based scenario recognition with multi-constellation gnss measurements on a smartphone. *Measurement*, 153, 107420.
- Zadeh, L. A. (1996). Fuzzy sets. In *Fuzzy sets, fuzzy logic, and fuzzy systems: Selected papers by lotfi a zadeh* (pp. 394–432). World Scientific.
- Zhu, H., Yuen, K. V., Mihaylova, L., & Leung, H. (2017). Overview of Environment Perception for Intelligent Vehicles. *IEEE Transactions on Intelligent Transportation Systems*, 18(10), 2584–2601. <https://doi.org/10.1109/TITS.2017.2658662>
- Zhu, Y., Luo, H., Zhao, F., & Chen, R. (2020). Indoor/outdoor switching detection using multisensor densenet and lstm. *IEEE Internet of Things Journal*, 8(3), 1544–1556.